Improved mobilities and resistivities in modulation-doped *p*-type AlGaN/GaN superlattices

Erik L. Waldron,[a] John W. Graff, and E. Fred Schubert
Department of Electrical and Computer Engineering, Boston University, Boston, Massachusetts 02215

(Received 1 May 2001; accepted for publication 21 August 2001)

The transport properties of modulation, shifted modulation, and uniformly doped $Al_{0.20}Ga_{0.80}N$/GaN superlattices are presented. The modulation-doped sample is doped only in the AlGaN barriers. The shifted-modulation-doped sample has its dopants shifted by one-quarter period. Measurements reveal a strong improvement in mobility and resistivity for the modulation-doped and shifted-modulation-doped structures versus the uniformly doped structure. The modulation-doped sample has a mobility of 9.2 and 36 cm^2/V s at 300 and 90 K respectively and a very low resistivity of 0.20 and 0.068 Ω cm at 300 and 90 K, respectively. Capacitance–voltage profiling shows multiple two-dimensional hole gases. The results are consistent with a reduction of neutral impurity scattering for modulation-doped structures as compared to uniformly doped structures. © *2001 American Institute of Physics.* [DOI: 10.1063/1.1410340]

Mg acceptors in GaN and $Al_xGa_{1-x}N$ have an activation energy of 150–250 meV,[1–3] much larger than kT at 300 K, resulting in low activation and therefore low conductivity in p-type GaN, degrading the performance of light-emitting diodes, lasers, and heterojunction bipolar transistors. The strong temperature dependence of the transport properties is problematic for device operation at high as well as low temperatures where carrier freeze out occurs. P-type $Al_xGa_{1-x}N$/GaN doped superlattices have been demonstrated to have higher acceptor activation[4–7] resulting in low resistivity. This can be further improved by minimizing ionized and neutral impurity scattering mechanisms through modulation doping.[5]

In this work, the effect of modulation doping in $Al_{0.20}Ga_{0.80}N$/GaN superlattices is investigated using Hall-effect and capacitance–voltage ($C-V$) profiling techniques. Mobility, resistivity, and carrier concentration are measured as a function of temperature. We show the modulation-doped (MD) and shifted-modulation-doped (SMD) samples to have superior electrical properties compared to uniformly doped (UD) samples, especially at low temperatures. Furthermore, $C-V$ profiles are presented that show the multiple two-dimensional hole gases (2DHGs) of the superlattice structure.

The Mg-doped gallium-faced superlattices (SLs) were grown by molecular-beam epitaxy on c-plane sapphire substrates. All doped regions have a Mg concentration of $N_{Mg} \approx 10^{19}$ cm^{-3} and all samples have an equal barrier and well width of 100 Å. This width is chosen to minimize the effects of growth irregularities and alloy scattering. The MD, SMD, and UD samples have 20, 20, and 15 periods, respectively. Only the barrier layers of the MD sample are doped whereas the well layers are undoped. The SMD sample is identical to the MD sample except that the SMD dopants are shifted one-quarter period away from the epilayer surface in order to maximize the separation of the dopants from the 2DHG. The UD sample has both the $Al_{0.20}Ga_{0.80}N$ barrier and GaN well layers doped. The doping profiles of all samples are shown in Fig. 1.

The variable temperature Hall-effect measurements are performed from 90 to 390 K in 10 K increments using the van der Pauw geometry. Pd/Au p-type ohmic contacts are deposited using electron beam evaporation. A CRYO Industries cryostat is used and the magnetic field is 0.5 T. The $C-V$ profile uses a mercury probe in conjunction with a HP

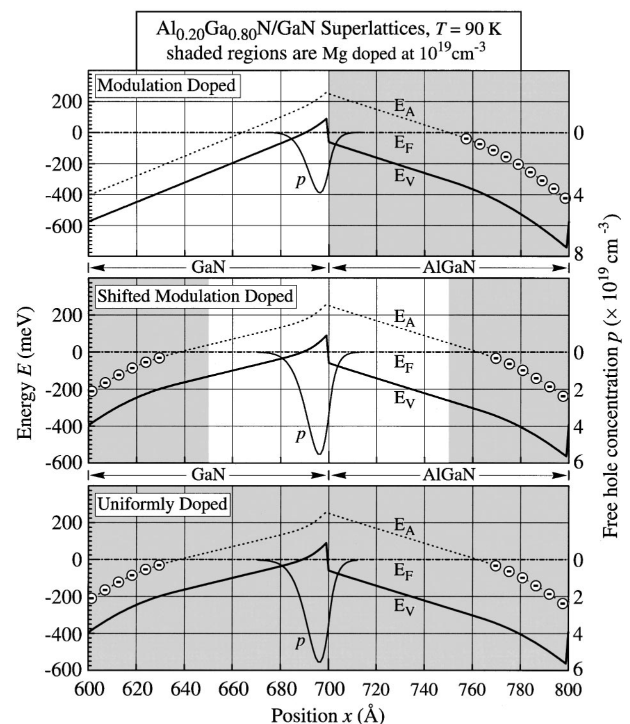

FIG. 1. Self-consistent valence band diagrams of a MD SL, a SMD SL, and a UD SL. The three ground state hole energies are $E_0 - E_F = -5.9$ meV, −1.7 meV, and −1.7 meV, respectively. P is the self-consistently solved free hole concentration. The ground state is the only occupied subband at 90 K. The epilayer surface is on the left-hand side.

[a]Also at: Department of Physics, Boston University, Boston, Massachusetts 02215; electronic mail: ewaldron@bu.edu

 © 2001 American Institute of Physics
Downloaded 18 Oct 2001 to 128.197.178.203. Redistribution subject to AIP license or copyright, see http://ojps.aip.org/aplo/aplcr.jsp

TABLE I. Hall effect data of doped $Al_{0.20}Ga_{0.80}N$/GaN SLs.

Parameter	MD	SMD	UD
300 K mobility (cm^2/V s)	8.9	5.6	3.0
90 K mobility (cm^2/V s)	36	18	2.0
300 K resistivity (Ω cm)	0.21	0.66	0.81
90 K resistivity (Ω cm)	0.068	0.21	0.84
300 K hole conc. ($\times 10^{18}$ cm^{-3})	3.4	1.7	2.6
90 K hole conc. ($\times 10^{18}$ cm^{-3})	2.5	1.6	3.7
Activation energy (meV) T=250 to 390 K	16	13	30

4194A Impedance/Gain-Phase Analyzer using a voltage sweep from 0 to 6 V. A low measurement frequency of 5 kHz is required to reduce the effects of parasitic series resistance.

SL structures use materials with different band gaps and, in the case of the III-nitrides, large internal polarization fields.[8–10] A bound surface charge results when $\mathbf{P}\cdot\hat{n}\neq 0$, where $\mathbf{P}$ is the polarization at the surface and $\hat{n}$ is the surface normal. A bound interface charge results when $\nabla\cdot\mathbf{P}\neq 0$, where $\mathbf{P}$ is the internal polarization. These occur at each interface within the SL. The result of the bound polarization charges and modulated band gap is a tilting of the valence band within the barriers and wells, as displayed in Fig. 1. Free holes are created when the acceptor level is near or below the Fermi level. Holes accumulate along those SL interfaces where the valence band is near the Fermi level, giving origin to a 2DHG.

The band diagrams in Fig. 1 are calculated self-consistently using a one-dimensional (1D) Schrödinger–Poisson solver.[11] An $Al_xGa_{1-x}N$ hole mass[9] of $(1.76+1.77x)m_{e,z}$, valence band discontinuity of 0.3 ΔE_g, and energy gap $E_g(x)=(3.425+2.71x)$ eV is used, x being the aluminum concentration. The calculated free hole concentration is shown in Fig. 1 for each type of SL. At 90 K, only the ground states are occupied. The Mg ionization energy in AlGaN is not known precisely. However, recent results have shown that the ionization energy of Mg acceptors in $Al_xGa_{1-x}N$ increases from ~170 meV to 360 meV for $x=0$ to $x=0.27$, respectively.[12,13] We therefore use a simple Vegard-like relationship and put the acceptor level, E_A, at $(170+704x)$ meV above the valence band. The calculated average free hole concentrations at 90 K are 2.3×10^{18} cm^{-3}, 3.3×10^{18} cm^{-3}, and 3.3×10^{18} cm^{-3} for the MD, SMD, and UD SL, respectively. This agrees favorably with the measured values given in Table I.

Figure 2 shows the hole mobilities of the three SL structures as a function of temperature. Inspection of Fig. 2 shows a large improvement in mobility for the MD and SMD SLs versus the UD SL, especially at low temperatures. Values of the hole mobility at selected temperatures are given in Table I. The mobility of the MD and SMD SLs continues to increase monotonically with decreasing temperature, indicative of the reduced influence of ionized impurity scattering. This mobility behavior along with a lack of carrier freeze out and the results of our simulation also suggest the presence of a 2DHG. The peak at 150 K and subsequent decrease in mobility for lower temperatures in the UD SL is characteristic of impurity scattering. All samples show a reduction of mobility at higher temperatures due to a combination of polar optical phonon scattering (Fröhlich interaction), acoustic phonon scattering, and piezoelectric scattering.[14] Because the GaN family is strongly polar and AlGaN/GaN superlattices contain strong polarization fields,[15] polar optical phonon scattering is expected to be the dominant scattering mechanism at temperatures above ~150 K.

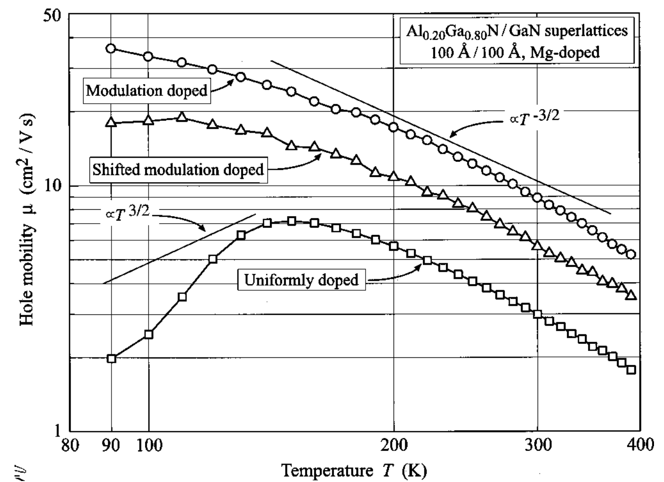

FIG. 2. Variable temperature hole mobility of a MD, a SMD, and a UD $Al_{0.20}Ga_{0.80}N$/GaN SL. Straight lines with $T^{3/2}$ and $T^{-3/2}$ dependencies represent impurity scattering and polar optical phonon scattering, respectively.

The reduction of neutral impurity scattering in the MD and SMD SL is expected since their 2DHG channels contain no intentional Mg dopants. The neutral dopants in the UD SL channels is shown to cause a sharp decrease in mobility at low temperatures $\propto T^{3/2}$. Note that the MD SL exhibits a clearly higher mobility and lower resistivity than the SMD SL sample. These differences are not yet fully understood and are subject to further investigations.[16]

The resistivity of the SL samples as a function of temperature is shown in Fig. 3. There is an improvement for the MD and SMD SLs compared to the UD SL. At 300 K, the resistivity is 0.20 Ω cm for the MD SL. The lowest resistivity of the MD SL occurs at 90 K and is 0.068 Ω cm, which is a very low resistivity for p-type GaN and $Al_xGa_{1-x}N$ material. Table I contains selected resistivity values. Particularly noteworthy is the resistivity of the MD and SMD SLs, which is lower than the UD SL at all temperatures and decreases monotonically with decreasing temperature, not exhibiting

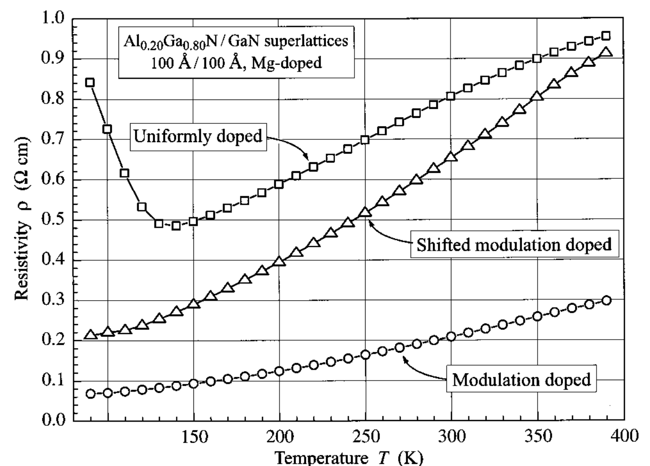

FIG. 3. Variable temperature resistivity data of a MD $Al_{0.20}Ga_{0.80}N$/GaN SL, a SMD $Al_{0.20}Ga_{0.80}N$/GaN SL, and a UD $Al_{0.20}Ga_{0.80}N$/GaN SL.

Downloaded 18 Oct 2001 to 128.197.178.203. Redistribution subject to AIP license or copyright, see http://ojps.aip.org/aplo/aplcr.jsp

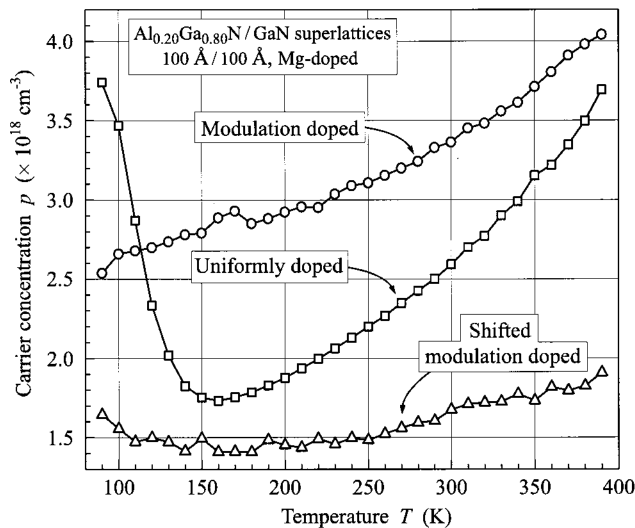

FIG. 4. Variable temperature three-dimensional carrier concentration data of a MD, a SMD, and a UD $Al_{0.20}Ga_{0.80}N$/GaN SL.

any freeze-out effect. This is due to the modulated valence band causing dopants to be ionized nearly independently of temperature. The improved resistivities demonstrated here should prove to be useful for the operation of GaN-based devices operating over a wide temperature range and underscore the importance of AlGaN/GaN superlattices.

The free hole concentration versus temperature is presented in Fig. 4, with tabulated values given in Table I for selected temperatures. The acceptor activation energies are 16 meV, 30 meV, and 13 meV for the MD, UD, and SMD SLs respectively, as determined in the temperature range of 250 to 390 K. These values are much smaller than activation energies of 200 meV found in bulk GaN.

$C-V$ measurements are presented in Fig. 5. The $C-V$ profile clearly shows the presence of a 2DHG with a peak at 390 Å and a full width at half maximum of 41 Å. This corresponds to a two-dimensional (2D) hole concentration of $\sim 4.9\times 10^{13}$ cm^{-2}, in reasonable agreement with the 300 K Hall value of 6.7×10^{13} cm^{-2}. The second peak at 690 Å shows the periodicity of the SL. The absolute position of the peaks is not as expected due to an uncertainty in material constants and a degradation of measurement phase angle. At positions greater than $\sim$800 Å, $C-V$ data cannot be obtained due to breakdown of the Hg probe Schottky contact.

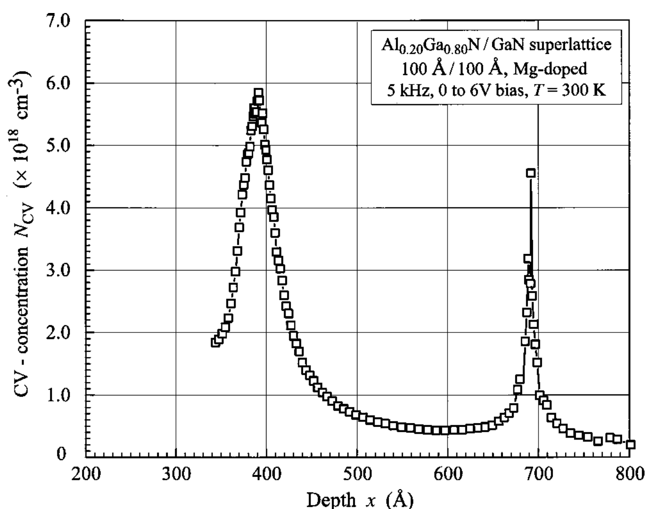

FIG. 5. $C-V$ concentration profile, N_{C-V}, versus depth of SMD $Al_{0.20}Ga_{0.80}N$/GaN SL.

In conclusion, we demonstrate improved mobilities and resistivities in MD and SMD $Al_{0.20}Ga_{0.80}N$/GaN SLs versus a UD SL. The lowest 300 and 90 K resistivities we obtain are for the MD SL and are very low for p-type $Al_xGa_{1-x}N$ material. The values are 0.20 Ω cm and 0.068 Ω cm, respectively. The lowest 300 and 90 K mobilities we obtain are also for the MD SL, and are 9.2 cm^2/V s and 36 cm^2/V s, respectively. Self-consistent calculations for all SLs show the formation of 2DHGs at the SL interfaces nearest the Fermi level. The improved mobilities of the MD and SMD SLs compared to the UD SL are consistent with a reduction of neutral impurity scattering in the wells of the MD and SMD samples. In addition, clear evidence of multiple 2DHGs is shown using $C-V$ profiling. The 2D hole concentration of 4.9×10^{13} cm^2 calculated from $C-V$ data is in reasonable agreement with the 300 K Hall effect value of the hole concentration.

This work was supported by the Office of Naval Research and monitored by Dr. C. E. C. Wood.

[1] H. Morkoç and S. Strite, J. Vac. Sci. Technol. B **10**, 1237 (1992).
[2] I. D. Goepfert, E. F. Schubert, A. Osinsky, and P. E. Norris, Electron. Lett. **35**, 1109 (1999).
[3] W. Götz, N. M. Johnson, J. Walker, D. P. Bour, and R. A. Street, Appl. Phys. Lett. **68**, 667 (1996).
[4] E. F. Schubert, W. Grieshaber, and I. D. Goepfert, Appl. Phys. Lett. **69**, 3737 (1996).
[5] P. Kozodoy, Y. P. Smorchkova, M. Hansen, H. Xing, S. P. DenBaars, U. K. Mishra, A. W. Saxler, R. Perrin, and W. C. Mitchel, Appl. Phys. Lett. **75**, 2444 (1999).
[6] A. Saxler, W. C. Mitchel, P. Kung, and M. Razeghi, Appl. Phys. Lett. **74**, 2023 (1999).
[7] P. Kozodoy, M. Hansen, S. P. DenBaars, and U. K. Mishra, Appl. Phys. Lett. **74**, 3681 (1999).
[8] F. Bernardini and V. Fiorentini, Phys. Rev. B **57**, 9427 (1998).
[9] N. Grandjean, B. Damilano, S. Dalmasso, M. Leroux, M. Laügt, and J. Massies, J. Appl. Phys. **86**, 3714 (1999).
[10] M. Leroux, N. Grandjean, M. Laügt, J. Massies, B. Gil, P. Lefebvre, and P. Bigenwald, Phys. Rev. B **58**, R13371 (1998).
[11] We used the freeware program *1D Poisson/Schrödinger* available at http://www.nd.edu/~gsnider/
[12] W. Götz, N. M. Johnson, J. Walker, D. P. Bour, H. Amano, and I. Akasaki, Appl. Phys. Lett. **67**, 2666 (1995).
[13] M. Stutzmann, O. Ambacher, A. Cros, M. S. Brandt, and H. Angerer, Mater. Sci. Eng., B **50**, 212 (1997).
[14] M. Shur, B. Gelmont, and M. Asif Khan, J. Electron. Mater. **25**, 777 (1996).
[15] E. L. Waldron, E. F. Schubert, J. W. Graff, A. Osinsky, M. J. Murphy, and W. F. Schaff, Materials Research Society Conference Proceedings, Boston, Massachusetts, 27 November–1 December, Fall 2000, Vol. 639.
[16] E. L. Waldron, J. W. Graff, and E. F. Schubert (unpublished).

Downloaded 18 Oct 2001 to 128.197.178.203. Redistribution subject to AIP license or copyright, see http://ojps.aip.org/aplo/aplcr.jsp